Aquatic Geochemistry (2023) 29:145–171
https://doi.org/10.1007/s10498-023-09414-3

ORIGINAL ARTICLE

Temporal and Seasonal Variations of Silicate Svratka River and Sediment Characterization, Czech Republic: Geochemical and Stable Isotopic Approach

Tjaša Kanduč[1] · Milan Geršl[2] · Eva Geršlová[3] · Jennifer McIntosh[4]

Received: 1 December 2022 / Accepted: 2 May 2023 / Published online: 18 May 2023

Abstract

This study investigated weathering and hydrobiogeochemical processes in a silicate dominated watershed (Svratka river) in the Czech Republic in comparison with nearby carbonate dominated catchments. Elemental and isotopic analysis of river waters, particulates and sediments provided a more holistic view of weathering contributions, anthropogenic contamination, biological activity and evasion or sinks of CO_2 to the atmosphere. In water samples, we determined total alkalinity after Gran 1974, and cations and anions were determined with inductively coupled plasma–optical emission spectrometer and ion chromatograph. $\delta^{13}C_{DIC}$ in water samples was determined with isotope ratio mass spectrometer. pCO_2 and saturation indexes of calcite and dolomite were calculated with PHREEQC speciation program. Evasion fluxes were calculated after Broecker, 1974. Isotopic composition of carbon and nitrogen in particulate matter and sediments were determined with isotope ratio mass spectrometer. Mineral composition of sediments was determined with XRD method and elements with XRF method. Further enrichment factors of elements were calculated. The Svratka river, which is the major tributary of the Dyje river, is dominated by $Ca^{2+} > Na^{+} > Mg^{2+} > K^{+}$ and HCO_3^{-} (as total alkalinity). Partial pressure (pCO_2) concentrations range from close to 0–572-fold of atmospheric pressure. Isotopic composition of carbon in dissolved inorganic carbon ($\delta^{13}C_{DIC}$) value ranged from − 13.3 to − 8.0‰ reflecting degradation of organic matter and exchange with the atmosphere. Bicarbonate weathering intensity for the Svratka river at its mouth is 11.8 mol/(l·km^2·s), more on par with silicate terrains and lower than nearby carbonate watersheds. Isotopic composition of carbon ($\delta^{13}C$) and isotopic composition of nitrogen ($\delta^{15}N$) values of river sediment reflect soil and temperate plant (C3 plant) values, while higher $\delta^{15}N$ values could be attributed to application of organic fertilizers in lower reaches. The river sediments, which came from weathering of crystalline rocks, are dominated by silt size, geochemically less mature quartz, feldspar and muscovite particles. All the stream sediments examined revealed slightly increased amounts of Zn, Cu and Pb. However, using Al as the normalization element to calculate enrichment factors, Zn, Cu and Pb are only elevated downstream, related to industrial contamination. This study is important for local and global level since it deals with contribution of weathering rates and contribution of CO_2 to the atmosphere in silicate watershed.

Extended author information available on the last page of the article

Keywords River systems · Silicate catchment · Stable isotopes · Mineral and elemental composition · Weathering intensity · Svratka river

1 Introduction

Combined evaluation of river water geochemistry and sediment composition provides important information on chemical weathering of bedrock/soils and natural and anthropogenic processes that may control the dissolved chemical load (Chougong et al. 2021; Lyons et al. 2021; Nasher and Ahmed 2021). It is known that chemical weathering of silicates is one of the major processes responsible for the transfer of dissolved and eventually particulate components from land to sea. The contributions of various rock types to the total dissolved load of world's rivers are estimated to be: 17% from evaporites, 38% from carbonates and 45% from silicates. This shows the significant role silicates play in overall chemical weathering of the earth surface. The rates of dissolution of silicates are very slow (Wollast and Chou 1988). Thus, carbonate weathering compared to silicate weathering largely dominates the chemistry of river waters (Gaillardet et al. 1999a, 1999b; Liu and Zhao 2000). However, studies of weathering intensity in silicate watersheds are also important for the estimation of overall weathering intensity and uptake of atmospheric CO_2 over geological timescales. Studying silicate weathering in a watershed adjacent to carbonate dominated watersheds previously studied provides an opportunity to compare weathering intensities in catchments with similar climates (Cai et al. 2020).

The application of stable isotopes and other geochemical approaches can provide important constraints on runoff, chemical weathering processes (Ben Othman et al. 1997; Cai et al. 2020) and different end-member solute sources, e.g. natural versus anthropogenic (Petelet-Giraud et al. 1998).

Rivers also reflect the biogeochemical processes occurring in their catchment areas, riparian zones and instream, and help to quantify material transport from the land to oceans (Palmer et al. 2001; Vázquez-Ortega et al. 2016; Li et al. 2017; Perdrial et al. 2018). The global riverine flux of dissolved inorganic carbon to the ocean is about 0.38×10^{15} g/yr (Meybeck 1993), similar in magnitude to the global riverine flux of organic carbon to the oceans, which is estimated to be 0.4×10^{15} g/yr (Meybeck 1982; Ittekot 1988). Riverine C represents a significant part of the global C budget since the total annual anthropogenic C input from fossil fuels is $5–6 \times 10^{15}$ g/yr (Berner and Berner 1996).

Within this context, understanding of the carbon cycle is particularly important because it helps to evaluate the health of the river and its catchment basin (Telmer and Veizer 1999). Carbon in rivers may occur as: dissolved inorganic carbon (DIC), dissolved organic carbon (DOC), particulate inorganic carbon (PIC) or particulate organic carbon (POC) (Cartwright 2010). Carbonate mineral dissolution and precipitation reactions generally dominate solute inputs to rivers and also play an important role in the transformation of terrestrial organic carbon in soils to inorganic carbon. Major elements and stable carbon isotopes of dissolved inorganic carbon ($\delta^{13}C_{DIC}$) are useful to constrain carbon sources and cycling (Karim and Veizer 2000; Barth et al. 2003; Kanduč et al. 2007a, 2008, 2017; Hagedorn and Cartwright 2010; Cartwright 2010; Cai et al. 2020). Stable carbon isotopic composition ($\delta^{13}C$) has been used in many studies to indicate whether carbonate dissolution by soil and atmospheric CO_2 is the major supplier of DIC in rivers (Dubois et al. 2010; Cai et al. 2015, 2020). Suspended organic matter in rivers is mostly derived from soil and plant material, and therefore, the isotopic composition of suspended organic matter ($\delta^{13}C_{POC}$) in rivers

has been used to ascertain the contribution of terrestrial vegetation and soil matter in the river ecosystem (Ittekot 1988; Hedges 1992; Kanduč et al. 2007b). Most soil organic matter (SOM) is plant-derived; only a small fraction of the yearly litter and root input becomes part of the stable organic matter pool, most of it after repeated processing by soil microorganisms (Six et al. 2004). The natural abundance of the ^{13}C and ^{15}N content in SOM is usually higher than that of the plant and fresh litter input (Amundson et al. 2003). Stable isotopes of carbon and nitrogen provide insight into biogeochemical processes occurring in the river. $\delta^{13}C_{org.}$ and $\delta^{15}N$ values in riverbed sediments derived from sewage and C3 plants range from − 27.2 to − 24.9‰· and from − 2.2 to + 10.9‰, respectively (Guo et al. 2020). Freshwater phytoplankton $\delta^{13}C$ and $\delta^{15}N$ values vary from − 35.0 to − 25.0‰ and from 5 to 8‰, respectively (Boutton 1991). Qualitative analysis indicates that there are four major sources of organic matter in studied sediment profiles: sewage, C3 plant, algae and soil organic materials (Guo et al. 2020).

Eutrophication and environmental pollution represent a serious issue in surface water systems worldwide, and sediment is the most dominant sink of environmentally released organic pollutants (Ke et al. 2017; Kubo and Kanda 2017). Excess nutrients and pollutants enter the fluvial system through natural processes, such as weathering, sheet wash and storm drains, as well as by those that include waste and sewage water washing, road runoff, atmospheric fallout and traffic. Thus, the chemical composition of river sediments represents the sum of the natural background and the anthropogenic load of the area (Sedláček et al. 2017; Vöröš et al. 2019). In the last decades, X-ray fluorescence (XRF) spectrometry is frequently used to measure major and trace elements in environmental samples and also in sedimentary units (Kern et al. 2019; Croudace et al. 2019; Laha et al. 2022). To assess the degree of environmental pollution, previous studies have used an enrichment factor (EF), which relates the concentration of elements in the river sediments compared to natural background levels (i.e. provenance effects) (Bábek et al. 2015; Nováková et al. 2015; Sakan et al. 2014; Matys-Grygar and Popelka 2016).

We hypothesize that the Svratka river is polluted; therefore, we applied mineralogical, e.g. XRD, XRF and isotopic, methods to evaluate its ecological state. The main objectives of the current study were to: (1) identify temporal and seasonal variations of major solutes in surface water and determine the sediment composition of the river Svratka; (2) evaluate and quantify riverine carbon sources, sinks and key biogeochemical processes in river water; (3) determine weathering intensity and evasion CO_2 flux; 4) determine carbon and nitrogen isotopic composition of particulate matter (PM); and (5) determine elemental composition of river sediment (RS) to evaluate possible anthropogenic load using the enrichment factor (EF) for selected elements (Zn, Cu, Pb, Cr and As).

2 Catchment Characteristics

The Svratka, formerly *Švarcava,* is a river in the South Moravian Region of the Czech Republic with a length of 173.9 km. It comes from the Bohemian-Moravian Highlands, converges with the Svitava at Brno and flows into the Dyje (*Thaya*) a few kilometres from Mikulov (Fig. 1). The Svratka river is sourced by springs, at an altitude of about 780 m above sea level.

The area of the Svratka river basin is 7,118.7 km^2, and the absolute slope of the river from the source area to the estuary is 613 m. Specific runoff is highest in the upper part of the basin (up to 11,9 $l{\cdot}s^{-1}{\cdot}km^{-2}$) and decreases downstream (Kestřánek and Vlček 1984).

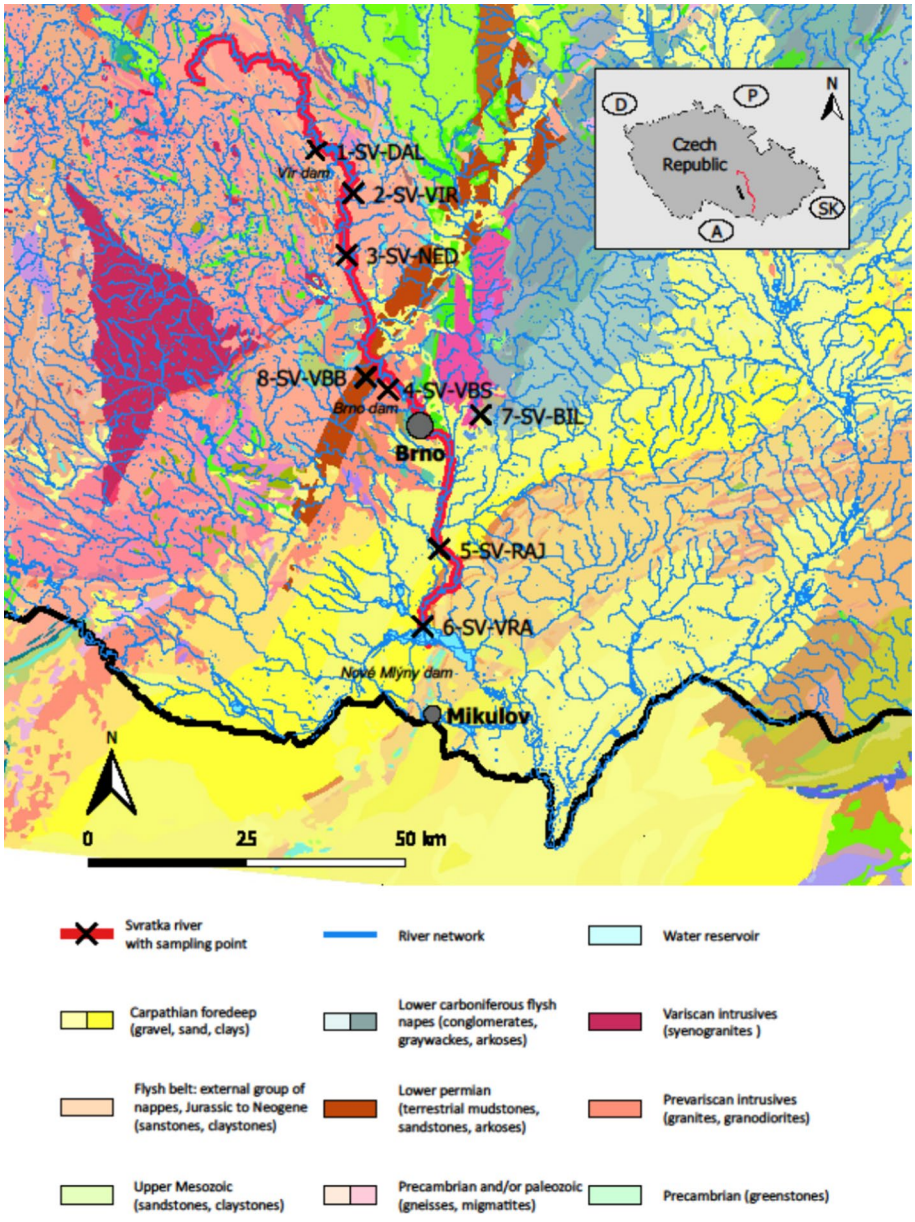

Fig. 1 Sampling points of the river Svratka (main channel and tributaries) with geological characteristics of catchment area

Svratka springs in the area where the river valley is 100–200 m wide and in some places narrows to a width of several tens of metres. On the upper course of the river, there is a dam reservoir Vír I, intended for drinking water with total volume 56.3 mil.m^3. Downstream situated Vír II is used as a buffer dam. A Kníničská (Brno) dam was built in 1954 in the narrow gorge above Brno. Dam was used as a drinking water source; now it is used

for energy production and to increase flows in the river Svratka. Below the dam, its largest tributary flows into the Svitava river and later, the second largest tributary of the Litava (Cezava) river. Finally, in the Nové mlýny reservoir, the Svratka river flows with the Dyje and Jihlava (Fig. 1).

2.1 Geological Settings

The geological conditions of the river Svratka basin are very diverse and include the metamorphic, igneous and sedimentary rocks. The upper stream flows through double-mica gneisses, then the area formed by crystalline rocks (Fig. 1). Subsequently, the Svratka river near Veverské Bitýška flows through the Lower Permian sediments of the Boskovice furrow and flows through the Brno city, whose surrounding is built of the Brno massif (diorite and granodiorite). Below Brno, the Svitava flows into the Svratka, and the river basin already flows through the area formed by the Miocene sediments of the Carpathian foredeep (Novák 1991).

The Svitava river basin has a more diverse geological composition as springs in the Cretaceous basin and flows through Permian sediments of the Boskovice Furrow. Before influence with the Svratka river it flows through the Brno massif and waters from the area draining Variscan flysch and Devonian limestone flow into it (Fig. 1).

2.2 Pedology

The upper Svratka river basin up to about Jimramov has shallow, stony soils. From Jimramov pod Tišnov, clayey–aluminous mica occurs on the crystalline base of the soil and sandy–loamy soils of gneisses, boulders and phyllites. The upper part of the Svitava river basin consists of heavy Cretaceous soils, mainly saliva (Fig. 1). The Boskovice furrow through Svitava and Svratka has medium type soils, i.e. ordinary clay and shallow stony soils (Fig. 1). The upper parts of the tributaries from the Drahanská Highlands have heavy soils of the North Moravian curling iron type (Novák 1991). The upper part of the basin Cezavy consists of light soils, humus and earthy sands, as well as heavy, impermeable Tertiary clays, formed on a flysch (Fig. 1) base extending from the watershed to almost the river itself.

3 Materials and Methods

3.1 Sampling Protocols and Field Measurements

Surface water sampling was performed along the river from the source to the confluence with the Jilhava river (Fig. 1). Sampling was performed at 6 locations in the main river channel and 2 tributaries (Table 1, Fig. 1) in different periods: two times in summer and two times in winter (January 2012 = winter, June 2012 = summer, December 2013 = winter, July 2014 = summer), according to the discharge regimes of river Svratka (Table 1). Discharges is higher in winter months ranging from 0.2 to 13.4 m^3/s and lower in summer months ranging from 0.0 to 5.8 m^3/s (Flood forecasting service, https://hydro.chmi.cz/hpps/index.php?lng=ENG). Water temperature, pH, ORP and electrical conductivity were measured using a WTW Multi 340i/SET, and oxygen saturation was determined with a

Table 1 Physical and chemical properties (average values in all sampling seasons: January 2012, June 2012, December 2013, July 2014) of surface waters of river Svratka

Numbers	Sample sites	Coordinates	Distance from the source (km)	Q (m^3/s)	T (° C)	pH	Conductivity (µS/cm)	Eh (mV)	DO (mg/l)
1	SV-DAL	49°35′31,7″ 16°25′23,8″	48.2	2.6	8.6	8.3	182.1	− 67.9	9.1
2	SV-VIR	49°33′35,2″ 16°18′35,4″	57.1	2.7	7.6	7.5	171.7	− 11.8	9.7
3	SV-NED	49°27′00,2″ 16°20′43,9″	78.4	3.3	9.0	7.4	294.3	− 14.5	9.6
4	SV-VBS	49°17′01,1″ 16°25′23,8″	102.4	5.1	11.2	7.7	332.0	− 36.9	10.3
5	SV-RAJ	49°05′02,3″ 16°37′11,5″	134.6	7.9	13.7	7.6	535.5	− 24.3	9.6
6	SV-VRA	48°57′03,7″ 16°37′09,6″	169.3	8.8	14.5	8.0	601.8	− 52.3	9.8
7	SV-BIL	49°16′14,1″ 16°25′40,2″	61	0.2	n.d	6.9	539.5	− 42.5	11.2
8	SV-VBB	49°14′22,9″ 16°40′00,9″	35	1.9	10.6	7.9	575.5	6.9	10.9

n.d.-not determined, 1–6–main channel, 7–8–tributaries (SV-BIL, SV-VBB)

GMH 3610 in the river water. The precision of dissolved oxygen saturation and conductivity measurements was ± 5%.

Sample aliquots collected for chemical analysis were passed through a 0.45 µm nylon filter into bottles and kept refrigerated until analysed. Samples for cation (treated with HNO_3), anion and alkalinity analyses were collected in HDPE bottles. Samples for $\delta^{13}C_{DIC}$ analyses were stored in glass serum bottles filled with no headspace and sealed with septa caps.

Samples for stable carbon isotope analysis of particulate organic carbon ($\delta^{13}C_{POC}$), particulate nitrogen ($\delta^{15}N$) and suspended matter were collected in LDPE bottles (Schuster and Reddy 2001). Sediments for $\delta^{13}C$ and $\delta^{15}N$ analyses were collected in plastic bags along river flow at the same locations as the river water samples.

Twenty-one samples of riverbed sediments were taken from the Svratka at the same time as water samples (Fig. 1, Table 1). The 4 samples were collected from the Svratka tributary Bílý potok (SV-VBB) and Svitava (SV-BIL) (Fig. 1). All the samples collected were homogenized, air-dried and sieved through a ~ 0.212 mm sieve. The prepared samples were stored in plastic bottles at room temperature for further analyses. The fine-grained sediments were preferably sampled to avoid the influence of grain size on element content.

3.2 Laboratory Analyses

Total alkalinity was measured by Gran titration (Gieskes 1974) with a precision of ± 1% within 24 h of sample collection. In order to measure alkalinity, the water sample was passed through a 0.45 m nylon filter into an HDPE bottle and kept refrigerated until analysed. Approximately 8 g of the water sample was weighed into a plastic container and

placed on a magnetic stirrer. A calibrated pH electrode (7.00 and 4.00 ± 0.02) was placed in the sample and the initial pH was recorded. Reagencon HCl 0.05 N (0.05 M) was used for titration. The titration performed using a CAT titrator (Ingenierbüro CAT, M. Zipperer GmbH Ballrechten-Dottingen, Germany).

Major ion chemistry was analysed in the Hydrology and Atmospheric Sciences Department at the University of Arizona (UA). Major cations (Ca, Mg, Na, K, Al, Si) were analysed (precision ± 2%) with a PerkinElmer Optima 5100DV inductively coupled plasma–optical emission spectrometer (ICP-OES), and some major anions (Cl^-, SO_4^{2-}, Br^-, F^-) were analysed (precision ± 2%) with a Dionex Ion Chromatograph (IC) Model 3000, using an AS23 analytical column.

The stable isotope composition of dissolved inorganic carbon ($\delta^{13}C_{DIC}$) was determined with an Isoprime 100 mass spectrometer coupled with the Multiflow preparation module (Elementar, Manchester, UK) at Jožef Stefan Institute. Phosphoric acid (100%) was added (100–200 µl) to a septum tube and then purged with pure He. The water sample (1 ml) was then injected into the septum tube and CO_2 was directly measured from the headspace after extraction (modified after Kanduč et al. 2007a). A standard solution of Na_2CO_3 (Carlo Erba) with a known $\delta^{13}C_{DIC}$ value of −10.8‰ ± 0.2‰ was used to control $\delta^{13}C_{DIC}$ measurements and perform normalization of measurements (Kanduč et al. 2007a, 2008).

To determine the mass of suspended matter a 0.7 µm pore size (GF/F) filters were used, which comprises CPOM (Coarse Particulate Organic Matter) and FPOM (Fine Particulate Organic Matter) (Devol and Hedges 2001). Filters were ignited before sampling at 480 °C with the aim of eliminating impurities, and then dried and weighed after filtering of suspended matter at Mendel University of Brno. The carbon stable isotope composition of particulate organic carbon ($\delta^{13}C_{POC}$) was determined with a Europa Scientific 20–20 continuous flow IRMS ANCA-SL preparation module at Jožef Stefan Institute. After sampling, one litre of the water sample was filtered through a Whatman GF/F glass fibre (0.7 µm). Filters were treated with 1 M HCl to remove carbonate material and then they were dried at 60 °C and stored until analyses. Approximately 1 mg of POM was scraped from the filter into a tin capsule. Approximately 10 mg of POM was scrapped from the filter (with no acid pre-treatment) for determination of isotopic composition of nitrogen ($\delta^{15}N$) at Jožef Stefan Institute. The isotopic composition of nitrogen and carbon was determined after combustion of the capsules in a hot furnace (temperature 1000 °C) (Kanduč et al. 2007b). Generated products were reduced in a Cu tube (600 °C), where excess O_2 was absorbed. H_2O was trapped on a drying column composed of $MgClO_4$. Gases were separated on a chromatographic column and ionized. NBS 22 (oil) and IAEA N-1 (ammonium sulphate) reference materials were used to relate the analytical results to the VPDB and AIR standards. The same way as we prepared samples for suspended matter isotopic analysis ($\delta^{13}C$ and $\delta^{15}N$) we prepared sediments.

All stable isotope results for carbon, nitrogen is expressed in the conventional delta (δ notation, defined as per mil (%) deviation from the reference standards VPDB, AIR. Precision was ± 0.2‰ for $\delta^{13}C_{DIC}$, $\delta^{13}C_{POC}$, $\delta^{13}C_{sediment}$, $\delta^{15}N_{sediment}$, $\delta^{13}C_{ca}$ and ± 0.3‰ for $\delta^{15}N$.

Thermodynamic computations were used to evaluate chemical speciation with the carbonate system (e.g. partial pressures of CO_2 (pCO_2), saturation indexes ($SI_{calcite}$, $SI_{dolomite}$, SI_{halite}, SI_{quartz}, $SI_{sylvite}$, SI_{talk}) of calcite ($CaCO_3$), dolomite ($CaMg(CO_3)_2$), halite (NaCl), quartz (SiO_2), sylvite (KCl) and talk ($Mg_3Si_4O_{10}$). Input parameters such as pH, alkalinity, temperature, and cation and anion concentrations were used as inputs to the PHREEQC speciation program (Parkhurst and Appelo 1999).

The bulk mineralogical composition was determined by homogenizing the 10 samples, grinding them in an agate mill to obtain a fraction below 0.2 mm at Technical university

Ostrava. All samples were prepared as texture free specimens (the surface was made coarse with sandpaper) and analysed using the Bruker D8 Advance diffractometer (CoKa/Fe radiation, 40 kV, 40 mA, step size: 014° 2q, 0.75 s, the measured interval being 2–80° 2q) with Lynxey's position-sensitive detector. Semiquantitative mineral estimates of the bulk sample were done using the Rietveld method (Bish and Post 1989) using the sw. Topasversion 4.2. with the accuracy of ± 10%.

The obtained fine-grained sediment was homogenized, dried at 105 °C, sieved to a fraction below 0.063 mm and ground in a mortar. The content of the elements (Si, Al, K, Ca, Ti, Zr, Rb, Th, Mn, Fe, Cr, Ni, Cu, Zn, As, Pb) was determined by the RFA method, using the Delta Premium instrument in Geochem mode at Masaryk university Brno. Reference materials Metranal 19, Metranal 34, Nist 2702, Nist 2781, IRM 5718 were used to verify the accuracy of the measurements.

The evasion of CO_2 from the river Svratka to the atmosphere $[DIC]_{ex}$ can be estimated based on the thin-film diffusive gas exchange model (Broecker 1974):

$$[\mathrm{DIC}]\mathrm{ex} = D/z \times ([\mathrm{CO_2}]_{\mathrm{eq}} - [\mathrm{CO_2}]) \quad (1)$$

where D is the CO_2 diffusion coefficient in water of 1.26 10^{-5} cm^2/s at a temperature of 10 °C and 1.67 $\cdot 10^{-5}$ cm^2/s at a temperature of 20 °C (Jähne et al. 1987), z is the empirical thickness of the liquid layer [cm], $[CO_2]_{eq}$ and $[CO_2]$ are the dissolved CO_2 concentrations at equilibrium with the atmosphere and with the studied water [mol·cm^{-3}], respectively. The thickness of the boundary layer z, a thin film existing at the air–water interface, depends on wind velocity (Broecker et al. 1978) and water turbulence (Holley 1977). D/z, therefore, is the gas exchange rate, which gives the height of the water column, which will equilibrate with the atmosphere per unit time. Using a mean wind speed of 4 m/s in both sampling seasons in the Svratka watershed, D/z was estimated to be 8 cm/h at low turbulence conditions, 28 cm/h at moderate turbulence conditions.

Data normalization was applied to the assessment of anomalous metal contribution using Al as a reference element. Data from the publication by Rudnick and Gao (2003) were used as the background values. The enrichment factor (EF) in river sediment was calculated according to following equation (Reimann and de Caritat 2005):

$$\mathrm{EF} = (A/An)/(B/\mathrm{Bn}) \quad (2)$$

A = The content of the element in the river sample.
An = The content of the normalized element in the river sample.
B = The content of the element in the background samples.
Bn = The content of the normalized element in the background samples.

4 Results

Sampling locations with underlying geology are presented in Fig. 1. Physical and chemical properties (T, pH, conductivity, DO) as well as distance from the source and discharge of the river (Q) is presented in Table 1. Temperature is lower in the upper reaches of the river (< 9.0 °C: Fig. 2a) and is to 1.6 °C, while in lower reaches average temperature of the river is up to 24.2 °C (Fig. 2a). pH is in the range from 5.7 to 8.7 and is lower at following locations: SV-VIR, SV-NED and SV-BIL in winter season. Average conductivity increases downstream from 168 µS/cm (upper reaches) to 695 µS/cm (lower reaches) (Fig. 2b). Dissolved oxygen (DO) is saturated (8.3 mg/l at 25 °C,

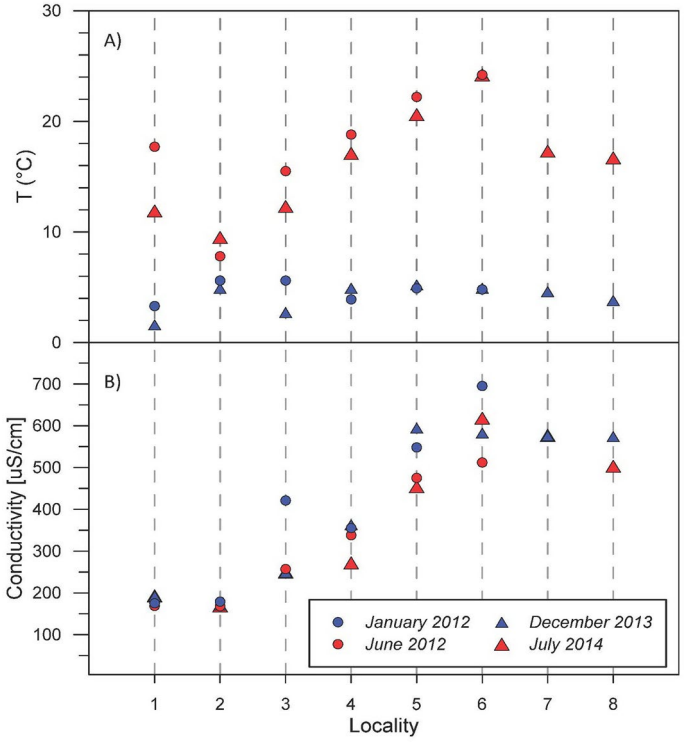

Fig. 2 **a** T versus locality, **b** Conductivity versus locality; location 1-SV-DAL, location 2-SV-VIR, location 3-SV-NED, location 4-SV-VBS, location 5-SV-RAJ, location 6-SV-VRA, location 7-SV-BIL, location 8-SV-VBB

Atkins 1994) all along the river and ranges from 5.8 to 13.1 mg/l. Generally the river is saturated with oxygen, except during the summer seasons June 2012 and July 2014 at SV-DAL, SV-NED, SV-VBS, SV-RAJ, SV-VRA and at SV-DAL and SV-VIR in July 2014. Detailed geochemical (saturation indices of minerals, e.g. quartz, talk, halite) and isotopic composition of dissolved inorganic carbon ($\delta^{13}C_{DIC}$) for each sampling season (January 2012, June 2012, December 2013 and July 2014) are presented in Supplementary material (Tables SM 1–4). Data are also uploaded to public repository (Kanduč et al. 2022). Alkalinity ranges in all seasons from 0.1 to 3.4 mM, while cation concentrations are as follows: Ca^{2+} from 0.39 to 1.95 mM, Mg^{2+} from 0.14 to 0.70 mM, Na^{+} from 0.30 to 1.69 mM and K^{+} from 0.05 to 0.2 mM (Tables SM 1–4). Anion concentrations vary as follows: Si from 0.15 to 0.25 mM, Al from 0.01 to 2.19 mM, Cl^{-} from 0.2 to 1.85 mM, SO_4^{2-} from 0.24 to 0.80 mM, Br^{-} from around 0 to 0.37 mM and SO_4^{2-} from 0.24 to 0.80 mM (Table SM 1–4). Partial pressure of CO_2 ranges from -5.0 to -0.64 bar meaning up to 573 times over saturated river if we take into account normal atmospheric pressure of 400 ppm (Tables SM 1–4). $\delta^{13}C_{DIC}$ values vary from -13.3% to -8.0‰ (Tables SM 1–4) with no significant trend seasonally and along the river. $SI_{calcite}$ range from -3.95 to 0.96, $SI_{dolomite}$ range from -8.6 to 1.5, SI_{halite} range from -9.9 to -0.3, SI_{quartz} range from -1.2 to 0.4, $SI_{sylvite}$ range from -8.6 to -7.5 and SI_{talk} range from -17.6 to 0.09 (Tables SM 1–4).

Isotopic results of $\delta^{13}C$ and $\delta^{15}N$ of particulate matter (PM) and river sediment (RS) are presented in SM Table 5. $\delta^{13}C_{POC}$ values range from − 29.7 to − 23.0‰, while $\delta^{15}N$ values range from + 6.0 to + 12.1‰. $\delta^{13}C$ values of river sediment vary from − 29.5 to − 24.8‰, while $\delta^{15}N$ values range from + 3.3 to + 8.8‰ (SM Table 5).

The content of the major mineral phases (in wt%) identified with XRD in Svratka river sediments for January 2012 and June 2012 sampling seasons is presented in Table 2 and the elemental content (µg/g) of river sediments (point 1–6 point) and its tributaries are reported in SM Table 6.

The major mineral phases detected include: quartz, feldspars (orthoclase and oligoclase) and muscovite. Calcite, actinolite and hornblende were also commonly detected (Table 2). The major and trace element composition of riverine sediments were (in order of concentration): Si > Al > Fe > K > Ca and Ti > Mn > Zr > Rb > Zn > Pb. The content of Th, Ni, Cu, As and Cr was negligible (Table SM 6). Results of enrichment factors (EF) calculated for Zn, Pb, Cu, As and Cr according to Eq. (2) are presented in Table SM 7 and range from 3.7 to 24.8 for Zn, from 2.8 to 9.5 for Pb, from 2.1 to 7.0 for Cu, from 0.5 to 1.4 for Cr and from 3.7 to 28.0 for As.

5 Discussion

5.1 Geochemistry of River Water

The pH of Svratka river water is highly variable ranging from 5.7 to 8.7, indicating that H_4SiO_4 is present in addition to HCO_3^-. Rock weathering (see equations from 3 to 6) contributes a significant portion of HCO_3^- to most world rivers and therefore strongly influences the riverine carbon cycle (Barth et al. 2003). In the case of silicate weathering of plagioclase (anorthite), two moles of HCO_3^- and one mole of Ca^{2+} are produced:

$$\underset{\text{(anorthite)}}{CaAl_2Si_2O_8} + 3H_2O + 2CO_2 \rightarrow \underset{\text{(kaolinite)}}{Al_2Si_2O_5(OH)_4} + Ca^{2+} + 2HCO_3 \quad (3)$$

In the case of albite weathering, Na^+ and HCO_3^- are produced in a 1:1 stocichometric ratio:

$$\underset{\text{(albite)}}{NaAlSi_3O_8} + CO_2 + 11/2\ H_2O \rightarrow Na^+ + 1/2\ \underset{\text{(kaolinite)}}{Al_2Si_2O_5(OH)_4} + 2H_4SiO_4 + HCO_3^- \quad (4)$$

Weathering of K-feldspar (microcline, orthoclase) to kaolinite releases 4 mol of SiO_2(aq) and two moles of K^+:

$$\underset{\text{(orthoclase, microcline)}}{2KAlSi_3O_8} + 2H^+ + H_2O \leftrightarrow \underset{\text{(kaolinite)}}{Al_2Si_2O_5(OH)_4} + 2K^+ + 4SiO_{2(aq)} \quad (5)$$

Weathering of Mg mineral (chlorite) produces 5 mol of Mg^{2+}, 10 mol of HCO_3^- and one mole of H_4SiO_4:

$$\underset{\text{(chlorite)}}{Mg_5Al_2Si_3O_{10}(OH)_8} + 10CO_2 + 5H_2O \leftrightarrow \underset{\text{(kaolinite)}}{Al_2Si_2O_5(OH)_4} + 5Mg^{2+}10HCO_3^- + H_4SiO_4 \quad (6)$$

Figure 3a shows that Svratka river water has $Ca^{2+} + Mg^{2+}$:HCO_3^- ratios closer to 1:1 indicating the weathering of oligoclase ((Na, Ca)[Al(Si, Al)Si_2O_8] is dominant.

Table 2 Content of the major mineral phases (in wt%) identified with XRD in river sediments of the Svratka river, others: calcite, actinolite, hornblendite

Locality ID	Season	Quartz	Feldspars	Muskovite	Chlorite	Others
1-SV-DAL	January 2012	51.9	11.5 (9.8 albite, 1.7 orthoclase)	34.9	0.7	1.0 (actinolite)
2-SV-VIR	January 2012	26.1	53.4 (32.9 orthoclase, 20.5 oligoclase)	19.8	0.7	0.0
3-SV-NED	January 2012	25.5	24.4 (5.3 orthoclase, 19.1 oligoclase)	49.8	0.3	0.0
4-SV-VBS	January 2012	30.5	18.1 (3.0 orthoclase, 15.1 oligoclase)	51.0	0.4	0.0
5-SV-RAJ	January 2012	36.6	21.3 (7.2 orthoclase, 14.1 oligoclase)	35.8	0.4	5.9 (hornblende)
6-SV-VRA	January 2012	59.6	18.8 (0.3 orthoclase, 18.5 oligoclase)	8.9	7.7	5.0 (calcite)
1-SV-DAL	June 2012	56.1	37.3 (28.4 oligoclase, 8.9 microcline)	2.9	2.5	1.2 (actinolite)
2-SV-VIR	June 2012	64.7	30.8 (21.0 oligoclase, 9.8 microcline)	2.5	0.0	2.0 (actinolite)
4-SV-VBS	June 2012	48.4	29.6 (19.6 oligoclase, 10.0 microcline)	10.5	10.4	1.1 (actinolite 0.6 and calcite 0.5)
6-SV-VRA	June 2012	67.6	21.1 (16.2 oligoclase, 4.9 microcline)	3.0	0.2	8.1 (actinolite 4.1 and calcite 4)

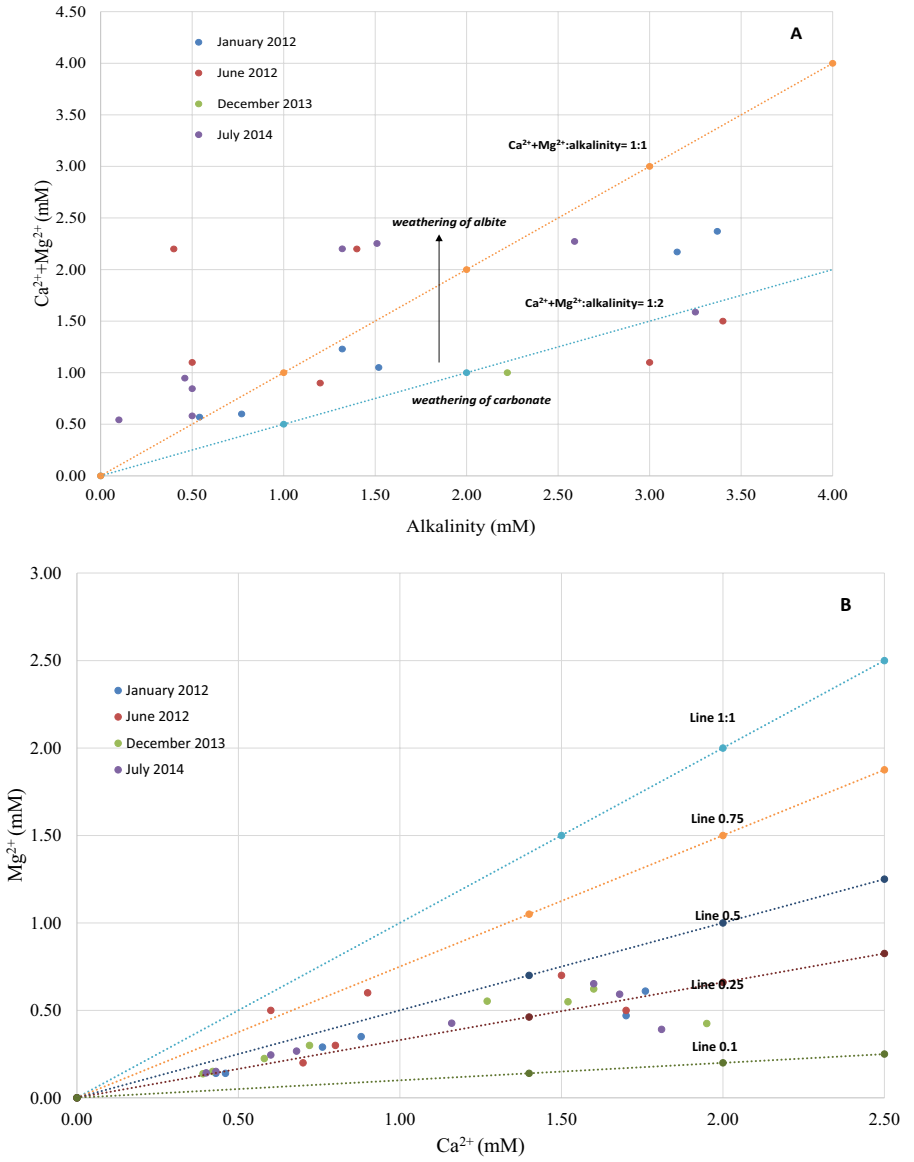

Fig. 3 **a** $Ca^{2+} + Mg^{2+}$ versus total alkalinity, **b** Mg^{2+} versus Ca^{2+}

In addition to other feldspars (orthoclase, microcline $KAlSi_3O_8$) (Table 2). It seems that among the feldspars albite (in general $Na^+ > Ca^{2+}$) prevails in the watershed and all feldspars weather to kaolinite (reactions 1–5).

In contrast, most rivers in nearby Slovenia (Szramek et al. 2007) have $Ca^{2+} + Mg^{2+}$:HCO_3^- ratio of 1:2 indicating the predominance of carbonate weathering controlling the geochemical composition of river water.

The molar ratio of Ca^{2+} ranges from 0.39 to 1.95 mM and Mg^{2+} from 0.14 to 0.70 mM, and the Mg^{2+}/Ca^{2+} ratio is less than 0.5, indicating that Ca^{2+} is the major cation in river water coming from weathering of feldspars and calcite (e.g. anorthite, oligoclase, hornblende, actinolite, calcite) (Table 2, Fig. 3b). Dolomite weathering leads to Mg^{2+}/Ca^{2+} ratios equal to or above 0.5. The dominance of calcite over dolomite weathering is also evident from the X-ray analysis (Table 2). The average Mg^{2+}/Ca^{2+} for river Svratka is 0.38 and ranges from 0.22 to 0.83. A Mg^{2+}/Ca^{2+} ratio of 0.33 is characteristic for rivers in the carbonate dominated Danube watershed (Szramek et al. 2007; Kanduč et al. 2013), such as the Sava, Tisa, Ilz and Inn rivers, while rivers in the more silicate dominated St. Lawrence watershed have Mg^{2+}/Ca^{2+} ratios > 0.33 (Szramek et al. 2007), which is similar to the river Svratka. Higher Mg^{2+}/Ca^{2+} ratios (above 0.5) in the river Svratka were observed at locations SV –RAJ and SV –VRA in June 2012, while all other samples locations had Mg^{2+}/Ca^{2+} ratios less than 0.5.

Thermodynamic modelling revealed that Svratka river waters were oversaturated with respect to calcite and dolomite (Fig. 4) in January 2012 and June 2012, while they were undersaturated in December 2013 and July 2014. Quartz and talc were undersaturated and oversaturated (saturation indices reported in Tables SM 1–4) in river waters, while halite and sylvite were undersaturated (Tables SM 1–4).

5.2 Carbon Cycling in River Svratka

Total alkalinity generally increases from the spring source downgradient in the river Svratka (Fig. 5a). There is a slight decrease in the alkalinity at sampling points 2 and 4, 57.1 km and 102.4 km, respectively, downstream. The upper reaches of the river Svratka have much lower total alkalinity (from 0.1 to 1.52 mM) compared to the lower

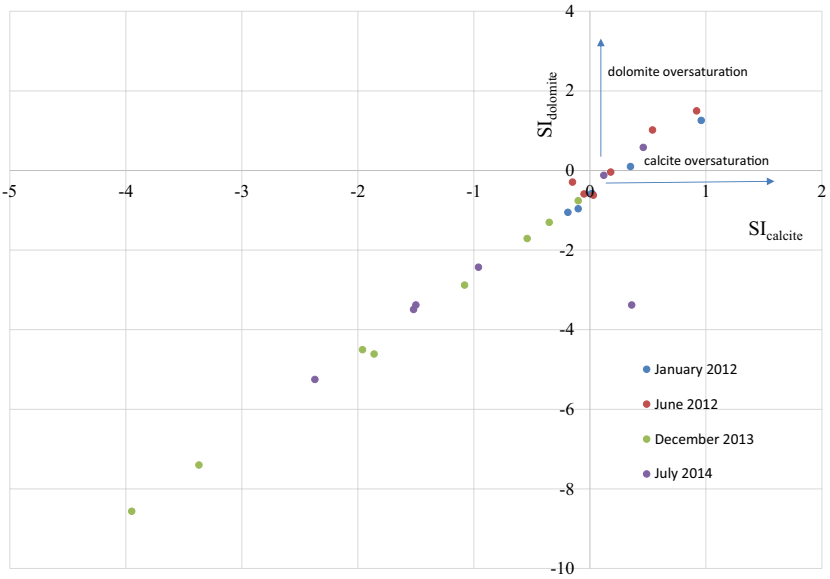

Fig. 4 $SI_{dolomite}$ versus $SI_{calcite}$

Fig. 5 **a** Alkalinity versus distance from the source, **b** $\delta^{13}C_{DIC}$ versus distance from the source, **c** $\delta^{13}C_{DIC}$ versus alkalinity with fractionation lines indicating major biogeochemical processes in river water, **d** pCO_2 versus distance from the source

reaches (1.32 to 3.40 mM). In January 2012 and June 2012, alkalinity continues to increase downstream, while in December 2013 and July 2014, there is a noticeable drop in alkalinity between the two lower most reach sampling points (5 and 6) (SV-RAJ) and SV-VRA, respectively). Those two low alkalinity measurements correspond to low discharge events in December 2013 and July 2014, while increases in January 2012 and June 2012. Figure 5 shows low alkalinities versus distance from the source due to low discharges in December 2013 and July 2014 (Tables SM 1–4). $\delta^{13}C_{DIC}$ values can help to decipher the following biogeochemical processes and contribution of DIC to the Svratka river: photosynthesis, degradation of organic matter and respiration, and equilibration with atmospheric CO_2. $\delta^{13}C_{DIC}$ is highly variable between locations and seasons along the river flow (Fig. 5b). In upper reaches, the highest $\delta^{13}C_{DIC}$ values in July 2014 and January 2012 are observed, while in June 2012 and December 2013 the lowest $\delta^{13}C_{DIC}$ values are detected. There is no obvious trend between $\delta^{13}C_{DIC}$ values and discharge in the river Svratka (Fig. 5b). The highest $\delta^{13}C_{DIC}$ value (-8.0‰) is observed at sampling location 3 (SV-NED) in July 2014. The lowest $\delta^{13}C_{DIC}$ value (-13.3‰) is observed in June 2012 also at the SV-NED location, probably due to more intense instream degradation of organic matter and leaching from terrestrial material into the river system.

Carbonate dissolution and its effect on $\delta^{13}C_{DIC}$ values was neglected in the Svratka river watershed since the watershed is mainly composed of feldspars and siliciclastic rocks (Fig. 1, Table 2).

The average Svratka river $\delta^{13}C_{POC}$ value of -27.2‰ (Table 3) was used to calculate carbon isotope fractionation lines shown in Fig. 6c. Open system equilibration of DIC with CO_2 from POC enriches DIC in ^{13}C by about 9‰ (Mook et al. 1974), which corresponds to -18.2‰. Given the isotopic composition of atmospheric CO_2 (-7.8‰, Levin et al. 1987) and the equilibration fractionation with DIC of $+9$‰, DIC in equilibrium with the atmosphere should have a $\delta^{13}C_{DIC}$ of about $+1.2$‰ (Fig. 5c). It seems that both biogeochemical processes (open system equilibration with the atmosphere and open system equilibration of DIC with soil CO_2 originating from degradation of organic matter) influence to $\delta^{13}C_{DIC}$ values of the Svratka river. If we consider two point sources, which contribute to $\delta^{13}C_{DIC}$; one coming from degradation of organic matter with value of -18.2‰ and the other from equilibration of CO_2 with value of CO_2 of $+1.2$‰ we can perform simple mass balance calculation. Since the watershed is composed of silicate rocks, dissolution of carbonates could be neglected. Soil CO_2 contribution seasonally change from 47.4 to 74.7% in summer season, while from 51 to 73.2% in winter season. Higher $\delta^{13}C_{DIC}$ values are observed in upper flow (0.5 km) in July 2014 (Fig. 5c), meaning that equilibration with atmosphere influence $\delta^{13}C_{DIC}$ values in water system.

Changes in partial pressure of CO_2 (pCO_2) are observed seasonally along the river flow (Fig. 5d). The lowest pCO_2 was measured in January 2012: at this time the river was a sink for CO_2. In July 2014, when the temperature was higher oversaturation with CO_2 occurred, probably also due to higher amounts of organic matter degradation.

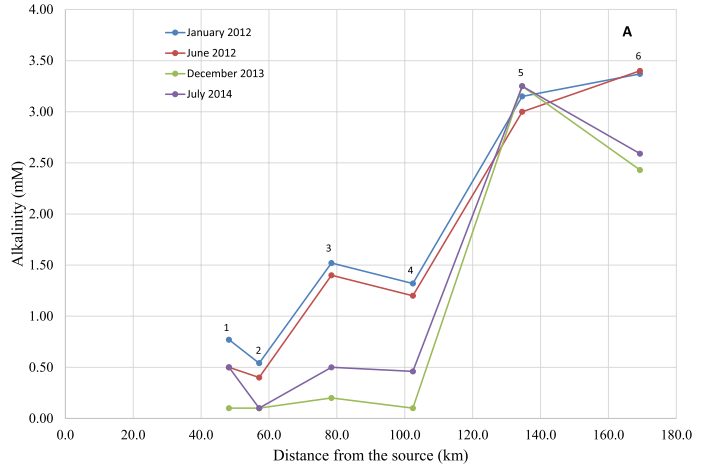
A
January 2012
June 2012
December 2013
July 2014
Alkalinity (mM)
Distance from the source (km)
1
2
3
4
5
6

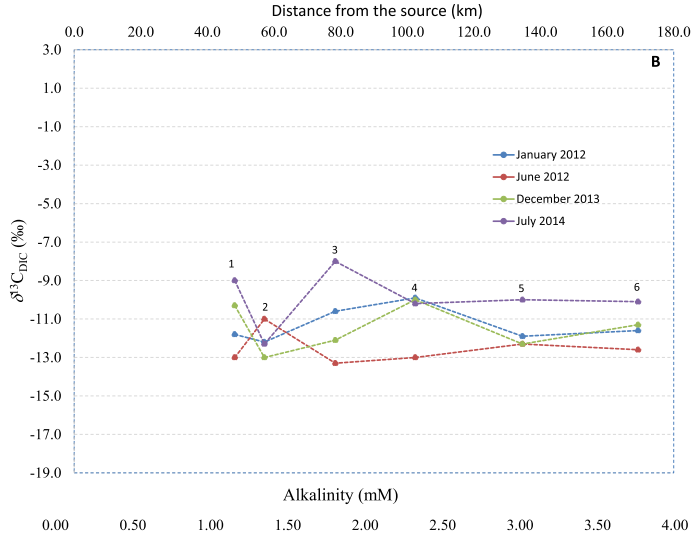
B
January 2012
June 2012
December 2013
July 2014
$\delta^{13}C_{DIC}$ (‰)
Alkalinity (mM)
1
2
3
4
5
6

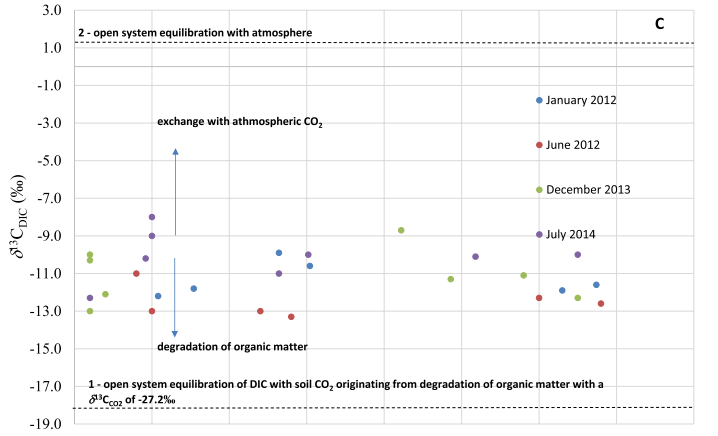
C
2 - open system equilibration with atmosphere
exchange with athmospheric CO_2
degradation of organic matter
1 - open system equilibration of DIC with soil CO_2 originating from degradation of organic matter with a $\delta^{13}C_{CO2}$ of -27.2‰
January 2012
June 2012
December 2013
July 2014
$\delta^{13}C_{DIC}$ (‰)

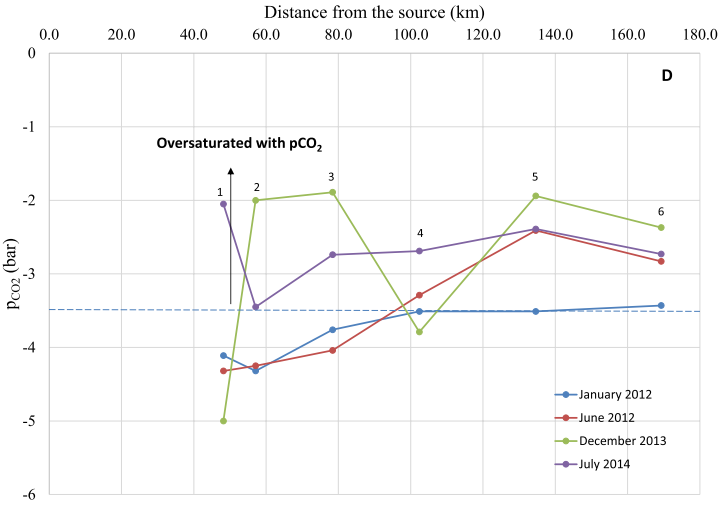

Fig. 5 (continued)

Table 3 $\delta^{13}C_{org}$ and $\delta^{15}N$ in soil, algae, atmospheric, *C*3 plants, *C*4 plants, sewage, literature data (average values, ranges and standard deviation—σ)

End-members	$\delta^{13}C_{org}$ (‰)	$\pm\sigma$	$\delta^{15}N$ (‰)	$\pm\sigma$
Soil	− 23.5, from − 22 to − 24	1.1	5.9, from 3 to 9	2.5
Algae	− 19.3, from − 14 to − 27	6.3	6.2, from 3 to 8	2.5
Atmospheric	− 24.5, from − 23 to − 26	1.7	− 2.1, from − 7 to 2	4.5
C3 plants[a]	− 28.5, from − 23 to − 30	0.5	4.5, from − 5 to 18	0.7
C4 plants[b]	− 15.3, from − 9 to − 17	4.2	5.8, from 3 to 6	2.4
Sewage[c]	− 25.3, from − 23 to − 28.5	2.75	from 7.0 to 25.0	

a—Kendall et al. 2001; Goni et al. 2003; Pancost and Boot (2004); Lamb et al. 2006; Yu et al. 2010; Gao et al. 2012; Lu et al. 2012, Gu et al. 2017, Rao et al., 2017, b—Deines (1980), Kendall et al. 2001; Gonni et al., 2003; Rao et al. 2017, c—Thornthon and McManus, 1994, Andrews et al. 1998, Liu et al. 2007, Machiwa 2010

5.3 Weathering Fluxes and Evasion CO_2 Flux of Svratka River

The major control on HCO_3^- weathering intensity is runoff (Holland 1978; Amiotte Suchet and Probst 1993). Weathering intensity normalized to drainage area quantifies HCO_3^- produced from mineral weathering (crystalline rocks) in the case of the Svratka river. Figure 7 presents HCO_3^- weathering intensity as a function of specific runoff for the Svratka watershed, combining new data from this study with published official data for the Sava river (largest river in Slovenia) and Idrijca river (EIONET 2005) and data from Berner and Berner 1996 for world rivers (7 mmol/l·km^2 ·s) and the Danube river. HCO_3^- weathering intensity for the Svratka river (SV–VRA location: site 6) is 11.8 mol/(l·km^2·s), which is closer to Mississippi and Danube rivers and characteristic for silicate weathering dominated watersheds, such as the Mississippi and Danube rivers, rather than the more carbonate weathering dominated Sava river with carbonate HCO_3^- weathering and its tributaries in Slovenia (37 to 140 mmol/(l· km^2· s). For example,

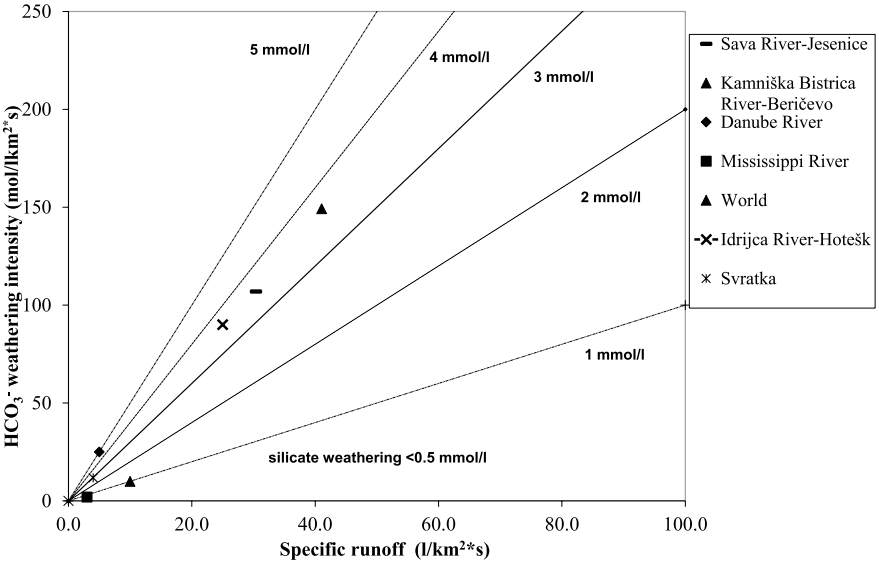

Fig. 6 Carbonate weathering intensity (HCO_3^- mmol/(l· km^2)) versus specific runoff indicating low carbonate weathering intensity in the Svratka watershed in comparison with other rivers in Slovenia and around the world. Data include mean long-term data of discharge and alkalinity from the Agency of the Republic of Slovenia of the Environment for Slovenian Rivers, and Berner and Berner 1996, for world rivers and the river Danube

the river Idrijca with torrential character at the Hotešk location in Slovenia has a much higher HCO_3^- weathering intensity of around 227 mmol/(l· km^2 ·s) (Kanduč et al. 2008).

The theoretical CO_2 diffusive evasion rates at all locations in all sampling seasons, according to Eq. 1, ranged between $1.77\cdot 10^{-8}$ and $1.37\cdot 10^{-6}$ mol/cm^2·h (low turbulence conditions) and $6.19\cdot 10^{-8}$ to $4.79\cdot 10^{-6}$ mol/cm^2 ·h (moderate to high turbulence conditions). Taking into consideration the river surface area of 4000 km^2 (mouth of the river Svratka at location SV-VRA). The estimated total diffusive loss of inorganic carbon varies seasonally (low conditions) and is estimated at location SV-VRA $2.9\cdot 10^4$ mol C/day in January 2012, $5.9\cdot 10^5$ mol C/day in June 2012, $2.2\cdot 10^6$ mol C/day in December 2013 and $8.0\cdot 10^5$·mol C/day in July 2014. The estimated total diffusive loss of inorganic carbon vary seasonally (moderate turbulent conditions) ranges from $1.0\cdot 10^5$ to $7.8\cdot 10^6$ mol C/day. Calculated total loss of inorganic carbon from the river surface ranged from a low as $6.6\cdot 10^5$ mol C/day to high as $1.2\cdot 10^6$ mol C/day during spring 2004 and are comparable to river Sava in Slovenia (Ogrinc et al. 2006). In comparison with the river Idrijca ($-2.55\cdot 10^3$ to $3.27\cdot 10^4$ mol C/day) in Slovenia (Kanduč et al. 2008) (up to $8.6\cdot 10^4$ mol C/ day at low conditions and up to $3.0\cdot 10^5$ mol C/day at high conditions) higher evasion CO_2 fluxes were calculated for the river Svratka. The evasion CO_2 flux is negative in the upper reaches of the river (undersaturated with CO_2) and in the January sampling season, while higher (oversaturated with CO_2) in lower reaches of the river and all seasons except in December 2013 (Fig. 5d).

Fig. 7 **a** $\delta_{13}C_{org.}$ of particulate matter (PM) and river sediment (RS) versus distance from the source, **b** δ_{15} N_{PM} and river sediment (RS) versus distance from the source, **c** δ_{15} N_{PM} versus $\delta_{13}C_{org}$ in particulate matter with comparison with soil, atmospheric, plants, sewage, algae (Guo et al. 2020; Table 3), **d** δ_{15} N_{RS} versus $\delta_{13}C_{org}$ in river sediments

5.4 Carbon and Nitrogen Isotopic Composition ($\delta^{13}C$ and $\delta^{15}N$) in Particulate Matter (PM) and River Sediments (RS)

From the plots (Fig. 7a and b), it is evident that $\delta^{13}C_{org.}$ and $\delta^{15}N$ values change seasonally in sediment and river sediment. The highest $\delta^{13}C_{org}$ values are detected in June 2012 (Fig. 7a) when degradation is the highest, while the lowest value is detected in December 2013. $\delta^{13}C$ values of river sediment samples fall between values of PM from December 2013 and June 2012 seasons (Fig. 7a). At sampling point 2 (SV-VIR) in January 2012 the highest $\delta^{15}N$ value is detected (12.1‰) at location SV-VIR (sampling point 2) (Fig. 7b). Table 3 presents $\delta^{13}C_{org}$ and $\delta^{15}N$ values for different end-members (soil, algae, atmospheric, plants and sewage) in environment. Those end-members are also presented in Fig. 7a and b to show comparison between particulate matter (PM) and river sediments (RS) in the river Svratka. Carbon and nitrogen isotopic values of river Svratka (Fig. 7a) and particulate matter (Fig. 7b) are characteristic for soil and particulate matter (Guo et al. 2020).

Higher $\delta^{15}N$ were measured in summer months at lower reaches of the Svratka river and indicate inputs of sewage sludge (Fig. 7b), while the lowest $\delta^{15}N$ values are detected in winter months. Lower $\delta^{15}N$ values are observed in river sediment in comparison with particulate matter and higher $\delta^{15}N$ values are generally detected at lower reaches in December 2013 sampling season with exception of SV-VIR (sampling point 2) (Fig. 7b). $\delta^{15}N$ values from literature data range from 7.0 to 25.0 (Table 3); therefore, we can conclude that elevated $\delta^{15}N$ values (above 7‰) indicate sewage contribution to riverine system.

Those end-members (Table 3) are also presented in Fig. 7c and d to show comparison between $\delta^{13}C$ and $\delta^{15}N$ values between particulate matter (PM) and river sediments (RS) of river Svratka system to decipher which end-member contributes the most. $\delta^{13}C$ values of river Svratka particulate matter fall between soil and C3 plants (Fig. 7c). $\delta^{13}C$ values of river sediment (Fig. 7d) fall close to soil and C3 plants similar as particulate matter. Some samples in particulate matter (SV-RAJ, SV-VBS, SV-VBB, SV-VRA) are enriched with ^{15}N isotope with $\delta^{15}N$ value close to 10‰ and probably indicate anthropogenic input–fertilizers or sewage sludge (Fig. 7d). Characteristic $\delta^{15}N$ value of soils ranges from 2.5 to 5.9‰ at the 0–50 cm depth, and the highest value (5.9‰) occurred at the 10–20 cm depth (Liu et al. 2021). Degradation of organic matter enriches RS and PM on ^{13}C isotope, similar as mineralization of organic matter enriches RS and PM with ^{15}N isotope. In general we obtain higher $\delta^{15}N$ values in particulate sediments than in river sediments from same location (Fig. 7b). Enrichment with heavier ^{15}N of particulate matter could be a result of degradation of organic matter along river flow. Besides mineralization also anthropogenic input enriches organic matter with ^{15}N isotope (Fig. 7c and d). Sewage sludge has $\delta^{15}N$ value up to 25‰ (Table 3, Fig. 7c and d). In our study most of the samples do not indicate severe anthropogenic pollution since both $\delta^{15}N$ values of particulate matter and river sediments indicate lower mineralization and low sewage input to river system. Further it is evident (Table 3) that algae and C4 plants have more positive $\delta^{13}C_{org.}$ values. For eutrophication $\delta^{13}C_{DIC}$ around 0‰ are characteristic (Karlović et al. 2022), but for river Svratka $\delta^{13}C_{DIC}$ are up to -8‰, meaning that eutrophication is not pronounced.

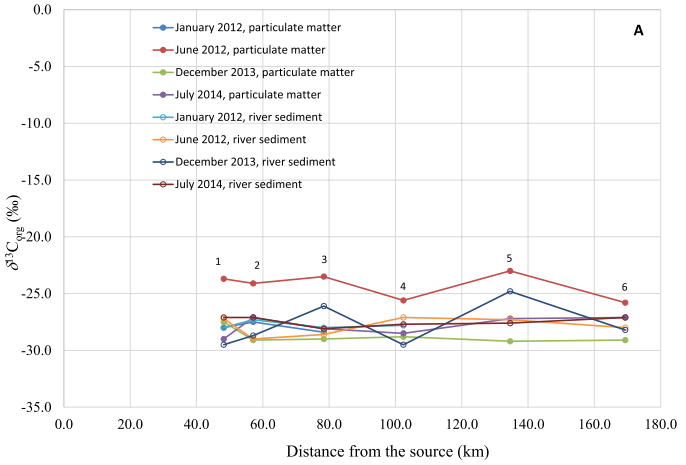
A
January 2012, particulate matter
June 2012, particulate matter
December 2013, particulate matter
July 2014, particulate matter
January 2012, river sediment
June 2012, river sediment
December 2013, river sediment
July 2014, river sediment
$\delta^{13}C_{org}$ (‰)
Distance from the source (km)

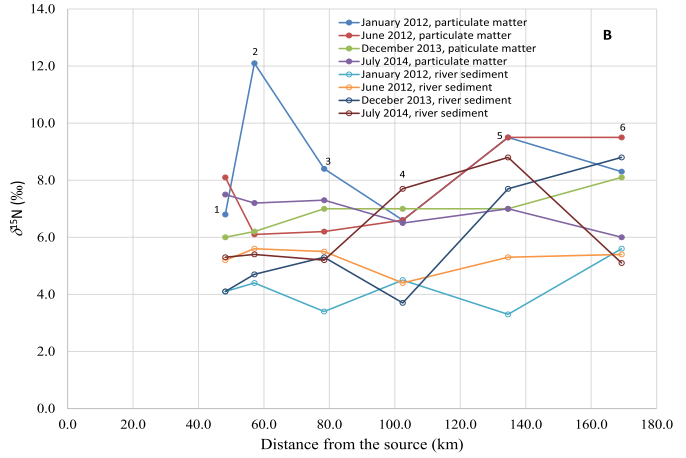
B
January 2012, particulate matter
June 2012, particulate matter
December 2013, paticulate matter
July 2014, particulate matter
January 2012, river sediment
June 2012, river sediment
Deceber 2013, river sediment
July 2014, river sediment
$\delta^{15}N$ (‰)
Distance from the source (km)

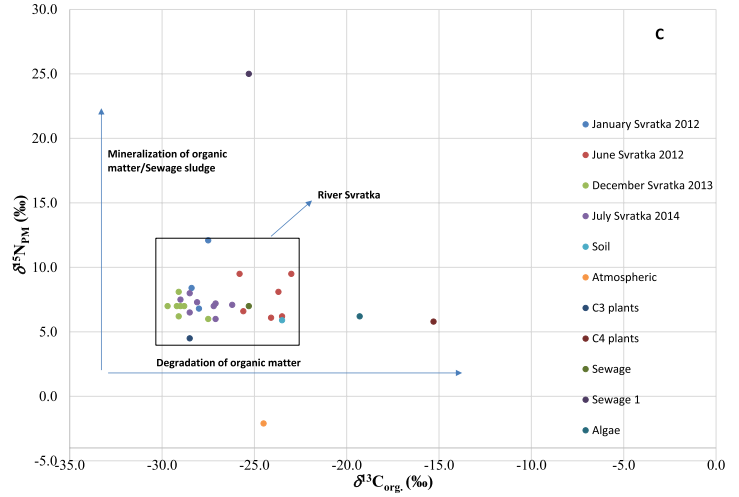
C
Mineralization of organic matter/Sewage sludge
River Svratka
Degradation of organic matter
January Svratka 2012
June Svratka 2012
December Svratka 2013
July Svratka 2014
Soil
Atmospheric
C3 plants
C4 plants
Sewage
Sewage 1
Algae
$\delta^{15}N_{PM}$ (‰)
$\delta^{13}C_{org.}$ (‰)

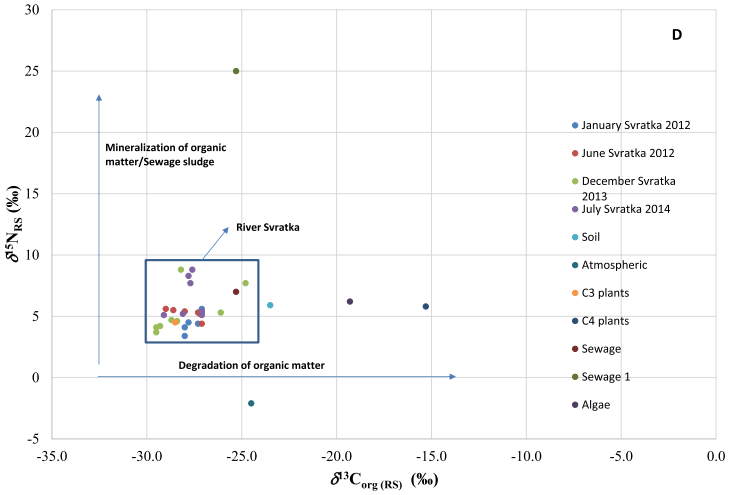

Fig. 7 (continued)

5.5 Sediment characterization of River Svratka Water System

The mineral composition of the river sediments is dominant by of quartz (25.5–67.6%, MED = 50.1%), feldspar (12.5–53.4%, MED = 25.8%) and muscovite (2.5–51.0%), which is consistent with the crystalline bedrock geology of the upper watershed (Fig. 1). Oligoclase is the most abundant of the feldspar group phases (MED 19.1%) and its origin is also as quartz related to crystalline rocks. Chlorite was the only clay mineral detected, its content varies from 0.2 to 10.4%, while one sample (2-SV-VIR) has no clay mineral fraction at all. Calcite was repeatedly detected in the last locality (6-SV-VRA) in slightly increased volume (4–5%).

Major elements in sediments of river Svratka are: Si > Fe > Al > Ca > K and trace elements: Ti > Mn > Zr > Zn > Rb > Cr > Cu > Pb > Ni > Th > As (SM Table 7). Elemental composition of the river sediments allowed more accurate interpretations as the major lithophile elements, Al, Si, Ti and Zr, are used as proxies of detrital components of sedimentary rocks. Ratios of these elements can provide information on the mineral composition and grain size, which are related to the provenance and intensity of chemical weathering (maturity) of the detrital component (Sageman and Lyons 2003). Al is usually bound in phyllosilicate minerals including feldspars and clay minerals, whereas Zr and Ti commonly indicate heavy minerals (zircons, titanites and rutiles). Si can be derived from detrital silicates or from terrestrial vegetation litter as the silica is forming phytoliths (Conley 2002) and also diatoms living in freshwater are important source of biogenic silica (Durr et al. 2011). The extreme concentrations of Mn, Fe, Cr, Ni, Cu, Zn were measured at location SV-VIR (sampling point 2).

Cross-plots (Fig. 8a and b) allow the visualization of the relationships between elements present in riverine sediments. Any positive correlations imply a likely association, while poor correlations indicate a different source or origin. The elemental cross-plots show strong positive correlation ($r = 0.87$) of Al and K (Fig. 8) for all samples excluding sample 2-SV-VIR from summer 2014 (Fig. 2a). This finding suggests that these elements came from weathering of mica and feldspars. Moreover, the strong

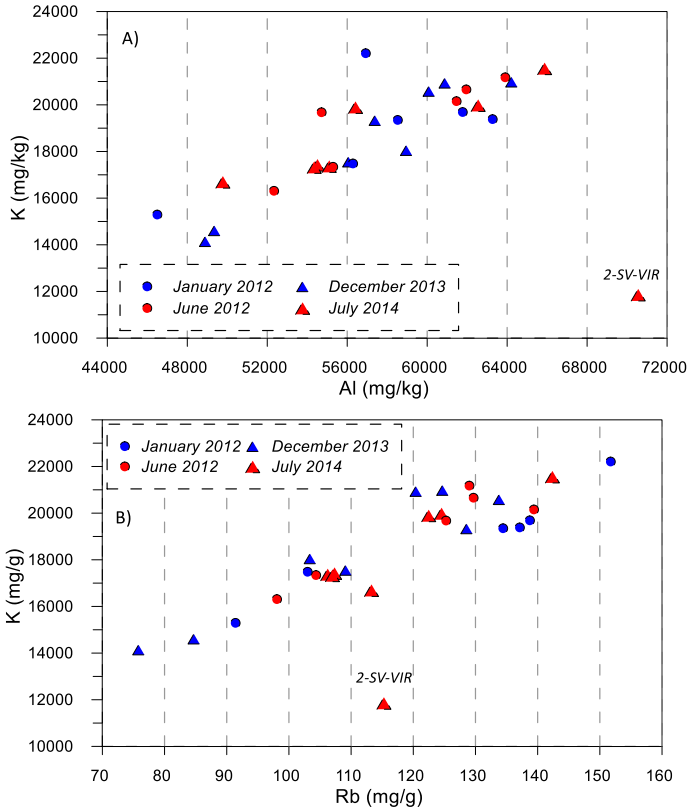

Fig. 8 **a** Potassium (K) versus aluminium (Al), **b** potassium (K) versus rubidium (Rb)

relationship between K and Rb (Fig. 8b) suggests that Rb is incorporated in muscovite as it is the dominant K-mineral along the river (Table SM 6).

The only exception is the sample 2-SV-VIR from summer 2014 with significant deficiency of K (11.851 mg/g), Si (176.468 mg/g) content but excess of Mn (16.593 mg/g), Fe (52.250 mg/g), Al (70.558 mg/g), Zn (1.437 mg/g) and Ni (0.111 mg/g) comparing to the whole evaluated set where the medium values are for Mn (12.37 mg/g), Fe (35.820 mg/g), Al (56.922 mg/g), Zn (0.258 mg/g) and Ni (0.035 mg/g). Such extreme values do not have a clear explanation, but may be associated with dam manipulation and are related release of sediments enriched with secondary minerals (Fe–Mn oxyhydroxides), which are formed in oxygen-deficient conditions. This assumption is consistent with lower content of Si and K and increased concentration of Mn, Fe, Cr, Ni, Cu and Zn. However, the presence of Fe-bearing minerals with associated trace elements cannot be excluded.

To evaluate the level of contamination in the Svratka river sediments the enrichment factor EF (Table SM 7) was calculated for Pb, Zn, Cu, Cr and As. Crystalline rocks form the Svratka upstream basin and therefore the values of the natural background of the upper crust for calculation of enrichment factor from Rudnick and Gao (2003) were chosen. In order to avoid influence of the sediment grain size on resulting pollution degree (Popelka and Grygar 2016), the Al was used as normalizing element. Al, Zr or Fe are generally accepted as conservative elements in riverine systems. However, in case of Svratka river

Zr seems to be related to the detrital fraction (correlation of Si and Zr 0.76). There are two large dams on the Svratka river and changes among oxic and anoxic conditions can be expected; thus, the use of Fe as a normalizing element does not appear to be beneficial.

Calculated values showed low EF values (Table SM 7) for Cr (not exceeding 1.4), highly variable values for As (3.7–28.1) with no obvious trend along the river. Since there are mentioned in historical occurrences of small ore fields in Svratka upstream watershed, it is possible that they are the source. A systematic increase in EF elements in Svratka river sediments along the stream was found for Zn, Cu and Pb for all monitored periods. The sampling points SV-RAJ and SV-VRA represents river after it flowed through the Brno city, have EF values of 6–10 for Zn, 3–7 for Pb and 4.1–7.0 for Cu, which are classified as moderately severe enrichment (Loska and Wiechula 2003). The point SV-VIR from July 2014 shows severe enrichment in As and Zn. The sample SV-VIR (sampling point 2 from July 2014 season is an outlier and does not represent river sediments (Fig. 8a and b). A long-term increased content of Pb, Cu and Zn in the sediments of the lower reaches of the Svratka river was found (SV-RAJ, SV-VRA), which is interpreted as the input of the mentioned elements from sources that are not related to the rock environment.

6 Conclusion

The major solute composition of the Svratka river is dominated by HCO_3^-, Ca^{2+}, Na^+, Mg^{2+}, K^+ and Cl^-. $\delta^{13}C_{DIC}$ values range from − 13.3 to − 8.0‰ and indicate: (1) exchange with atmospheric CO_2 and open system equilibration of DIC and (2) soil CO_2 originating from degradation of organic matter with $\delta^{13}C_{POC}$ of − 27.2‰. Based on thermodynamic modelling, Svratka river represents a source of CO_2 to the atmosphere, except in January and June 2012 in upper reaches. Higher $\delta^{13}C_{POC}$ is observed in summer months, probably due to higher degradation of organic matter from leached material from the surface. Bicarbonate weathering intensity of the Svratka river is 11.8 mol/(l· km^2 ·s) and is typical for silicate rivers worldwide.

Higher $\delta^{15}N$ values of particulate matter and sediments were detected in lowland Svratka sampling points in summer months due to low discharge. Higher $\delta^{15}N$ values are attributed to application of fertilizers in the watershed and are more pronounced in lower reaches. At lower reaches increased EF for zinc, copper and lead was found. It is highly probably not a single industrial source, but a number of small sources that combined after the river flows through the Brno agglomeration. X-ray diffraction results, including positive correlation of Al with K and Rb, show that quartz, feldspars (oligoclase) and muscovite are the dominant minerals in river sediments, reflecting the silicate composition of the watershed. Weathering of these minerals within the watershed contributes to total alkalinity and solute composition of river waters. Evaluation of river sediment, particulate organic carbon and solutes provided a more complete understanding of weathering, biogeochemical and anthropogenic processes within the river systems.

Major ion chemistry and stable isotopes as applied here and in previous studies shown are useful tracers of biogeochemical processes and anthropogenic influences in watershed providing a tool for water resource management. Herein we present data of $\delta^{13}C$ and $\delta^{15}N$ in river water, particulate matter and sediment environmental matrixes, which are additional tracers of pollution in watersheds. The element evaluation also demonstrated importance of using independent analytical methods to characterize samples. Study results are

also useful to provide background information on aquatic geochemistry in case of future management of the Svratka river system.

Supplementary Information The online version contains supplementary material available at https://doi.org/10.1007/s10498-023-09414-3.

Acknowledgements The authors are grateful to Mr. Stojan Žigon for technical support and isotopic analyses, to the programme research group "Cycling of nutrients and contaminants in the environment, mass balances and modelling environmental processes and risk analysis" (P1-0143), and research project (L1-5451) and Slovenian–American bilateral project 2012-2013 (BI-US/12-13-039): "Fluid dynamics and carbon cycling in sedimentary basins: geochemical characterization, evolution of biogeochemical processes and modelling" founded by Slovenian Research Agency. Part of the research was carried out thanks to the institutional support of the Faculty of Agriculture, Mendel University in Brno and Masaryk University in Brno. Tim Corley is acknowledged for analysing cation and anion chemistry of water samples.

Author contributions TK contributed to conceptualization. TK, MG, EG and JM were responsible for methodology, formal analysis and investigation, writing—original draft preparation, writing—review and editing, funding acquisition and resources. JM was involved in supervision.

Declarations

Competing interests The authors declare no competing interests.

References

Amiotte Suchet P, Probst JL (1993) Modelling of atmospheric CO_2 consumption by chemical weathering of rocks: application to the garonne, congo and Amazon basins. Chem Geol 107:205–210

Amundson R, Gao Y, Gang P (2003) Soil diversity and land use in the United States. Ecosyst 699(6):470–482

Andrews JE, Greenaway AM, Dennis PF (1998) Combined carbon-isotope and C/N ratios as indicators of source and fate of organic matter in a poorly flushed, tropical estuary-hunts Bay, Kingston Harbor Jamaica. Estuar Coast Shelf Sci 46:743–756

Atkins PW (1994) Physical chemistry. Oxford University Press, Oxford

Bábek O, Grygar TM, Faměra M, Hron K, Nováková T, Sedláček J (2015) Geochemical background in polluted river sediments: How to separate the effects of sediment provenance and grain size with statistical rigour? CATENA 135:240–253. https://doi.org/10.1016/j.catena.2015.07.003

Barth JAC, Cronin AA, Dunlop J, Kalin RM (2003) Influence of carbonates on the riverine carbon cycle in an anthropogenically dominated catchment basin: evidence from major elements and stable carbon isotopes in the Lagan River (N. Ireland). Chem Geol 200:203–216

Ben Othman D, Luck JM, Tournoud MG (1997) Geochemistry and water dynamics : application to short-time scale flood phenomena in a small Mediterranean catchment. I- alkalis, alkali-earths and Sr isotopes. Chem Geol 140:9–28

Berner EK, Berner RA (1996) Global environment, water, air, and geochemical cycles. 720 prentice hall. Upper Saddle River, New Jersey

Bish DL, Post JE (1989) Modern powder diffraction. Mineralogical society of America, Washington

Boutton TW (1991) Stable carbon isotope ratios of natural materials: II. Atmospheric, terrestrial, marine, and freshwater environments. In: Coleman DC, Fry B (eds) Carbon isotopes techniques. Academic Press, San Diego, pp 173–185

Broecker WS (1974) Chemical oceanography. In: Leeder MR (ed) Sedimentology and sedimentary basins. Harcout-Brace-Jovanovich, New York, p 592
Broecker HC, Peterman J, Siems W (1978) The influence of wind on CO_2–exchange in a wind–wave tunnel, including the effects of monolayers. J Mar Res 36:595–610
Cai Y, Guo L, Wang X, Aiken G (2015) Variations in the abundance and stable isotopic composition of DOC, POC, and DIC in the lower Mississippi River during 2006–2008. J Geophy Res Biogesciences 120:2273–2288
Cai Y, You CF, Wu SF, Cai WJ, Guo L (2020) Seasonal variations in strontium and carbon isotope systematics in the Lower Mississippi River: Implications for chemical weathering. Chem Geol 553:119810
Cartwright I (2010) The origins and behavior of carbon in a major semi-arid river, the Murray River Australia as constrained by carbon isotopes and hydrochemistry. Appl Geochem 738(25):1734–1745
Chougong DT, Bessa AZEB, Ngueutchova G, Yongue RF, Ntyah SC, Armstrong-Altrin JS (2021) Mineralogy and geochemistry of Lobé River sediments, SW Cameroon: Implications for provenance and weathering. J African Earth Sci 183:104320
Conley DJ (2002) Terrestrial ecosystems and the global biogeochemical silica cycle. Global Biogeochem Cy 16(4):1121. https://doi.org/10.1029/2002GB001894,2002
Croudace IW, Löwemark L, Tjallingii R, Zolitschka B (2019) Current perspectives on the capabilities of high resolution XRF core scanners. Quat Int 514:5–15. https://doi.org/10.1016/j.quaint.2019.04.002
Deines P (1980) The isotopic composition of reduced carbon. In: Fritz P, Fontes, JC (Eds), Handbook of environmental isotope geochemistry. vol 1. The Terrestrial Environment A, pp 329–406
Devol AH, Hedges JI (2001) Organic matter and nutrients in the mainstem amazon river. In: McClain ME, Victoria RL, Richey JE (eds) The biogeochemistry of the amazon Basin. Oxford University Press, New York, p 365
Dubois KD, Lee D, Veizer J (2010) Isotopic constraints on alkalinity, dissolved organic carbon, and atmospheric carbon dioxide fluxes in the Mississippi River. J Geophys Res Biogeosci 115:G2018. https://doi.org/10.1029/2009JG001102
Durr HH, Meybeck M, Hartmann J, Laruelle GG, Roubeix V (2011) Global spatial distribution of natural riverine silica inputs to the coastal zone. Biogeosciences 8:597–620. https://doi.org/10.5194/bg-8-597-2011
EIONET (2005) European environment information and observation network. http://eionet-en.arso.gov.si. Cited 11 Nov 2005
Gaillardet J, Dupre B, Allegre CJ (1999a) Geochemistry of large river suspended sediments: silicate weathering or recycling tracer? Geochim Cosmochim Acta 63:4037–4051
Gaillardet J, Dupre B, Louvat P, Allegre CJ (1999b) Global silicate weathering and CO_2 consumption rates deduced from the chemistry of large rivers. Chem Geol 159:3–30
Gao X, Yang Y, Wang C (2012) Geochemistry of organic carbon and nitrogen in surface sediments of coastal Bohai Bay inferred from their ratios and stable isotopic signatures. Mar Pollut Bull 64:1148–1155
Gieskes JM (1974) The alkalinity-total carbon dioxide system in seawater. In: Goldberg ED (ed) Marine Chemistry of The Sea, vol 5. John Wiley and Sons, New York, pp 123–151
Goni MA, Teixeira MJ, Perkey DW (2003) Sources and distribution of organic matter in a river-dominated estuary (Winyah Bay, SC, USA). Estuar Coast Shelf Sci 57:1023–1048
Gu YG, Ouyang J, Ning JJ, Wang ZH (2017) Distribution and sources of organic carbon, nitrogen and their isotopes in surface sediments from the largest mariculture zone of the eastern Guandong coast. South China, Mar Pollut Bull 120:286–291
Guo Q, Wang C, Wei R, Zhu G, Cui M, Okolic CP (2020) Qualitative and quantitative analysis of source for organic carbon and nitrogen in sediments of rivers and lakes based on stable isotopes. Ecotoxicol Environ Saf 195:110436
Hagedorn B, Cartwright I (2010) The CO_2 system in rivers of the Australian Victorian Alps: CO_2 evasion in relation to system metabolism and rock weathering on multi-annual time 794 scales. Appl Geochem 25:881–899
Hedges JI (1992) Global biogeochemical cycle: progress and problem. Mar Chem 39:67–93
Holland HD (1978) The chemistry of the atmosphere and oceans. Wiley, Hoboken, p 351
Holley EH (1977) Oxygen transfer at the air–water interface. In: Gibbs RJ (ed) Transport processes in lakes and oceans, Proc. Symp. On Transp. Processes in the Ocean held at the 2nd Nat. Meet Of the AICE, Atlantic City, N. J. Aug. 29.–Sep. 1, 1976, pp 117–150
https://hydro.chmi.cz/hpps/index.php?lng=ENG, Flood forecasting service (internet source) Cited Nov 2022
Ittekkot V (1988) Global trends in the nature of organic matter in the river suspensions. Nature 332:436–438
Jähne B, Heinz G, Dietrich W (1987) Measurments of the Diffision Coefficients of sparingly soluble gases in water. J Geophysical Res 92:10767–10776

Kanduč T, Szramek K, Ogrinc N, Walter LM (2007a) Origin and cycling of riverine inorganic carbon in the Sava River watershed (Slovenia) inferred from major solutes and stable carbon isotopes. Biogeochemistry 86:137–154. https://doi.org/10.1007/s10533-007-9149-4

Kanduč T, Ogrinc N, Mrak T (2007b) Characteristics of suspended matter in the River Sava watershed, Slovenia. Isot Environ Health Stud 43(4):369–385

Kanduč T, Kocman D, Ogrinc N (2008) Hydrogeochemical and stable isotope characteristics of the river Idrijca (Slovenia), the boundary watershed between the Adriatic and Black seas. Aquat Geochem 14:239–262

Kanduč T, Burnik Šturm M, McIntosh J (2013) Chemical dynamics and evaluation of biogeochemical processes in alpine river Kamniška Bistrica, North Slovenia. Aquat Geochem 19:323–346

Kanduč T, Kocman D, Verbovšek T (2017) Biogeochemistry of some selected Slovenian rivers (Kamniška Bistrica, Idrijca, and Sava in Slovenia): insights into river water geochemistry, stable carbon isotopes and weathering material flows. Geologija 60(1):9–26

Kanduč T, Geršl M, Geršlová E, McIntosh J (2022) Data of temporal and seasonal variations of silicate Svratka river and sediment characterization, Czech Republic: geochemical and stable isotopic approach, Mendeley Data, v1 https://doi.org/10.17632/x43d7tcwck.1DOI

Karim A, Veizer J (2000) Weathering processes in the Indus River Basin: implications from riverine carbon, sulfur, oxygen and strontium isotopes. Chem Geol 170:153–177

Karlović I, Marković T, Kanduč T, Vreča P (2022) Assessment of seasonal changes on the carbon cycle in the critical zone of a surface water (SW)–groundwater (GW) system. Water 14(21):3372. https://doi.org/10.3390/w14213372

Ke Z, Tan Y, Huang L, Zhao C, Jiang X (2017) Spatial distributions of delta(13)C, delta(15)N and C/N ratios in suspended particulate organic matter of a bay under serious anthropogenic influences: Daya Bay, China. Mar Pollut Bull 114:183–191

Kendall C, Silva SR, Kelly VJ (2001) Carbon and nitrogen isotopic compositions of particulate organic matter in four large river systems across the United States. Hydrol Process 15:1301–1346

Kern OA, Koutsodensis A, Mächte B, Christanis K, Schukroft G, Scholz C, Kotthoff U, Pross J (2019) XRF core scanning yields reliable semiqauntitative data on elemental composition of highly organic rich sediments: evidence from the Füramos peat bog (Southern Germany). Sci Total Environ 697:134110

Kestřánek J, Vlček V (1984) Watercourses and reservoirs-Geographical lexicon of Czech Republic, Academia Praha 314 pp (in Czech)

Kubo A, Kanda J (2017) Seasonal variations and sources of sedimentary organic carbon in Tokyo Bay. Mar Pollut Bull 114:637–643

Laha F, Gashi F, Frančišković-Bilinski S, Bilinski H, Çadraku H (2022) Geospatial distribution of heavy metals in sediments of water sources in the Drini i Bardhë river basin (Kosovo) using XRF technique. Sustain Water Resour Manag 8:31. https://doi.org/10.1007/s40899-022-00602-7

Lamb AL, Wilson GP, Leng MJ (2006) A review of coastal paleoclimate and relative sea-level reconstructions using $\delta^{13}C$ and C/N ratios in organic material. Earth Sci Rev 75:29–57

Levin I, Kromer B, Wagenback D, Minnich KO (1987) Carbon isotope measurements of atmospheric CO_2 at a coastal station in Antartica. Tellus B 39:89–95

Li L, Maher K, Navarre-Sitchler A, Druhan J, Meile C, Lawrence C, Moore J, Perdrial J, Sullivan P, Thompson A, Jin L, Bolton EW, Brantley SL, Dietrich EE, Mayer KU, Steefel CI, Vallocchi A, Zachara J, Kocar B, McIntosh J, Tutolo BM, Kumar M, Sonnenthal E, Bao C, Beishan J (2017) Expanding the role of reactive transport models in critical zone processes. Earth Sci Rev 165:280–301

Liu Z, Zhao J (2000) Contribution of carbonate rock weathering to the atmospheric CO_2 sink. Environ Geol 39:1053–1058

Liu KK, Kao SJ, Wen LS, Chen KL (2007) Carbon and nitrogen isotopic compositions of particulate organic matter and biogeochemical processes in the eutrophic Danshuei Estuary in northern Taiwan. Sci Total Environ 382:103–120

Liu M, Hou G, Li X (2021) Using stable nitrogen isotope to indicate soil nitrogen dynamics under agricultural soil erosion in the Mun River basin, Northeast Thailand. Ecol Ind 128:107814

Loska K, Wiechula D (2003) Application of Principal component analysis fort he estimation of source of heavy metal contamination in surface sediments from Rybnik Reservoir. Chemosphere 51:723–733

Lu F, Liu Z, Ji H (2012) Carbon and nitrogen isotopes analysis and sources of organic matter in the upper reaches of the Chaobai River near Beiing. China Sci China Earth 56:217–227

Lyons WB, Carey AE, Gardner CB, Welch SA, Smith DF, Szynkiewicz A, Diaz MA, Croot P, Henry T, Flynn R (2021) The geochemistry of Irish rivers. J Hydrol Reg Stud 37:100881

Machiwa JF (2010) Stable carbon and nitrogen isotopic signatures of organic matter sources in near -shore areas of Lake Victoria. East Africa J Great Lake Res 36:1–8
Matys-Grygar T, Popelka J (2016) Revisiting geochemical methods of distinguishing natural concentrations and pollution by risk elements in fluvial sediments. J Geochem Explor 170:39–57
Meybeck M (1982) Carbon, nitrogen, and phosphorus transport by world rivers. American J Sci 282:401–450
Meybeck M (1993) Riverine transport of atmospheric carbon: sources, global typology and budget. Water Air Soil Pollut 70:443–463
Mook WG, Bommerson JC, Staverman WH (1974) Carbon isotope fractionation between dissolved bicarbonate and gaseous carbon dioxide. Earth Planet Sci Lett 22:169–176
Nasher NMR, Ahmed MdH (2021) (2021): Groundwater geochemistry and hydrogeochemical processes in the Lower Ganges-Brahnaputra-Meghna River Basin area Bangladesh. J Asian Earth Sci X 6:100062
Nováková T, Matys Grygar T, Kotková K, Elznicová J, Strnad L, Mihaljevič M (2015) Pollution assessment using local enrichment factors: the Berounka River (Czech Republic). J Soils Sediments 16:1081–1092. https://doi.org/10.1007/s11368-015-1315-z
Ogrinc N, Kanduč T, Vaupotič J (2006) Isotopic characteristics of the Sava River basin in Slovenia. Radioact Environ 8:317–325. https://doi.org/10.1016/S1569+4860(05)08025-3
Palmer SM, Hope D, Billett MF, Dawson JJC, Bryant CL (2001) Sources of organic and inorganic carbon in a headwater stream: evidence from carbon isotope studies. Biogeochem 52:321e338
Pancost RD, Boot CS (2004) The paleoclimatic utility of terrestrial biomarkers in marine sediments. Mar Chem 92:239–261
Parkhurst DL, Appelo CAJ (1999) User's guide to PHREEQC (version 2)–a computer program for speciation, batch–reaction one–dimensional transport, and inverse geochemical calculations. Water Resources Invest Rep 99:4259
Perdrial J, Brooks PD, Swernam T, Lohse KA, Rasmussen C, Litvak M, Harpold AA, Zapata-Rios X, Broxton P, Mitra B, Meixner T, Condon K, Huckle D, Stielstra C, Vázquez-Ortega A, Lybrand R, Holleran M, Orem C, Pelletier J, Choroveer J (2018) A net ecosystem carbon budget for snow dominated forested headwater catchments: linking water and carbon fluxes to critical zone carbon storage. Biogeochem 138(3):225–243
Petelet-Giraud E, Luck JM, Ben Othman D, Négrel Ph, Aquilina L (1998) Geochemistry and water dynamics on a medium sized watershed: the Herault, S France. Chem Geol 150:63–83
Rao Z, Guo W, Cao J, Shi F, Jiang H, Li C (2017) Relationship between the stable carbon isotopic composition of modern plants and surface soils and climate: a global review. Earth Sci Rev 165:110–119
Reimann C, de Caritat P (2005) Distinguishing between natural and anthropogenic sources for elements in the environment: regional geochemical surveys versus enrichment factors. Sci Total Environ 337(1–3):91–107
Rudnick LR, Gao S (2003) Composition of the continental crust. Treatise Geochem 3:1–64. https://doi.org/10.1016/B0-08-043751-6/03016-4
Sageman BB, Lyons TG (2003) Geochemistry of fine-grained sediments and sedimentary rocks. Treatise Geochem. https://doi.org/10.1016/b0-08-043751-6/07157-7
Sakan S, Dević G, Relić D, Anđelković I, Sakan N, Đorđević D (2014) Evaluation of sediment contamination with heavy metals: the importance of determining appropriate background content and suitable element for normalization. Environ Geochem Health 67:97–113. https://doi.org/10.1007/s10653-014-9633-4
Schuster PF, Reddy MM (2001) Particulate Carbon (PC) and Particulate Nitrogen (PN). In: Water and sediment quality in the Yukon River Basin, alaska, during water year, Open-file report 03–427, National research program, USGS, available online: http://pubs.usgs.gov/of/2003/ofr03427/
Sedláček J, Bábek O, Nováková T (2017) Sedimentary record and anthropogenic pollution of a complex, multiple source fed dam reservoirs: An example from the Nové Mlýny reservoir. Czech Republic Sci Total Environ 1(574):1456–1471
Six J, Bossuyt H, Degryze S, Denef K (2004) A history of research on the link between (micro) aggregates, soil biota, and soil organic dynamics. Soil Tillage Res 79:7–31
Novák P (eds) (1991) Synthetic soil map of the Czech Republic. Atlas map 1:200000.–Ministry of Agriculture of the Czech Republic and Ministry of the Environment of the Czech Republic, Praha
Szramek K, McIntosh JC, Williams EL, Kanduč T, Ogrinc N, Walter LM (2007) Relative weathering intensity of calcite versus dolomite in carbonate-bearing temperature zone watersheds: carbonate

geochemistry and fluxes from catchments within the St. Lawrance and Danube river basin. Geochem Geophys Geosys 8:1–26
Telmer K, Veizer J (1999) Carbon fluxes, pCO_2 and substrate weathering in a large northern river basin, Canada: carbon isotope perspectives. Chem Geol 159:61–86
Vázquez-Ortega A, Perdrial J, Harpold A, Zapata-Rios X, Craig R, McIntosh J, Schaap M, Pelletier JD, Brooks PD, Amistadi MK, Chorover J (2016) Rare earth elements as reactive tracers of biogeochemical weathering in forested rhyolitic terrain. Chem Geol 391:19–32
Vöröš D, Geršlová E, Nývlt D, Geršl M, Kuta J (2019) Assessment of geogenic input into Bilina stream sediments (Czech Republic). Environ Monit Assess 191:2. https://doi.org/10.1007/s10661-019-7255-0
Wollast R, Chou L (1988) Rate control of weathering of silicate minerals at room temperature and pressure. In: Lerman A, Meybeck M (eds) Physical and chemical weathering in geochemical cycles. Kluwer Academic Publishers, Boston USA, pp 11–32
Yu F, Zong Y, Lloyd JM, Huang G, Leng MJ, Kendrck C, Lamb AI, Yim WWS (2010) Bulk organic δ13C and C/N as indicators for sediment sources in the Pearl River delta and estuary, southern China. Estuar Coast Shelf Sci 87:618–630

Authors and Affiliations

Tjaša Kanduč[1] · Milan Geršl[2] · Eva Geršlová[3] · Jennifer McIntosh[4]

✉ Tjaša Kanduč
tjasa.kanduc@ijs.si

Milan Geršl
gersl@mendelu.cz

Eva Geršlová
gerslova@mail.muni.cz

Jennifer McIntosh
jenmc@arizona.edu

[1] Department of Environmental Sciences, Jožef Stefan Institute, Jamova Cesta 39, 1000 Ljubljana, Slovenia

[2] Department of Agricultural, Food and Environmental Engineering, Faculty of AgriSciences, Mendel University in Brno, Zemědělská 1, 613 00 Brno, Czech Republic

[3] Department of Geological Sciences, Faculty of Science, Masaryk University, Kotlarska 2, 611 37 Brno, Czech Republic

[4] Department of Hydrology and Atmospheric Sciences, University of Arizona, 1133 E. James E, Rogers Way, Tucson, AZ 85721, USA